Biophysical Chemistry 5 (1976) 327–337


# SCANNING GEL CHROMATOGRAPHY: DETERMINATION OF TRANSPORT PARAMETERS FROM DYNAMIC PROFILES MEASURED AT LOW SOLUTE CONCENTRATION*

Maryann M. JONES‡, G. Arthur HARVEY, and Gary K. ACKERS
*Department of Biochemistry, University of Virginia, Charlottesville, Va. 22901, USA*

Received 3 March 1976

Direct optical scanning of solute boundaries in large zone gel chromatography experiments provides an accurate means of determining boundary profile shapes and rates of motion. A method has been developed for correcting such boundaries to a constant time frame, eliminating the distortion which arises from finite column scanning rate. Centroids of the corrected profiles can be used to determine the partition cross section for the solute of interest. The partition cross section and flow rate determine translational motion within the column. The axial dispersion coefficient, $L$, which characterizes rate of boundary spreading may also be calculated from the profiles. In order to explore these procedures a study of four noninteracting solutes was conducted. Partition cross sections determined from rates of motion of boundary centroids were found to be in good agreement with those determined by the equilibrium saturation method on the same column. In order to explore the lowest concentration limits of the technique and to illustrate the boundary characteristics for a self-associating solute, a study of carboxyhemoglobin was conducted over a wide concentration range. From measurements at 220 nm the lowest concentration where useful data could be obtained was 2 micrograms per ml (0.12 $\mu$M heme). These results establish validity of the procedures used in analyzing the rates of boundary transport and in studying solute transport over a wide range of conditions.

## 1. Introduction

Direct optical scanning of solute profiles in gel chromatography experiments provides a means to acquire a large amount of experimental information rapidly [1–4]. The feasibility of such measurements was initially demonstrated by Brumbaugh and Ackers [1] and the basic transport characteristics of solute zones and boundaries were surveyed. Subsequent studies [2–4] have been aimed at development of the equilibrium saturation technique in which solute profiles within the column are time-independent. The equilibrium technique affords the most accurate determination of solute partition cross sections and partition coefficients. It is from these experimental quantities that the molecular size and interaction parameters are most readily derived [5]. However, in spite of the high accuracy and theoretical simplicity inherent in equilibrium experiments, valuable additional information is contained in the time-dependent properties of solute profiles in transport experiments. This is particularly true in the case of solutes undergoing chemical reactions such as self-association [6–10]. The new technique of active enzyme chromatography, described in accompanying papers [11,12], also makes use of dynamic profiles. Consequently, we have undertaken a series of studies on the analysis of dynamic profiles experimentally obtained in direct optical scanning of gel chromatography experiments.

In this paper we describe the experimental determination and analysis of boundaries in "large zone" transport experiments† with single-species solutes (as a function of molecular size) and of simple self-associating systems. We have developed methods for accurate determination of profile centroids. Results will be presented illustrating their use in determining solute

* Supported by Grant GM-14493 from the National Institutes of Health.
‡ Part of this work is taken from the Ph.D. dissertation of Maryann M. Jones, August 1975.

† In this and the accompanying papers [11,12] we have used terminology and definitions developed previously and used consistently throughout the series of studies. A recent review containing detailed descriptions and definitions is ref. [5].

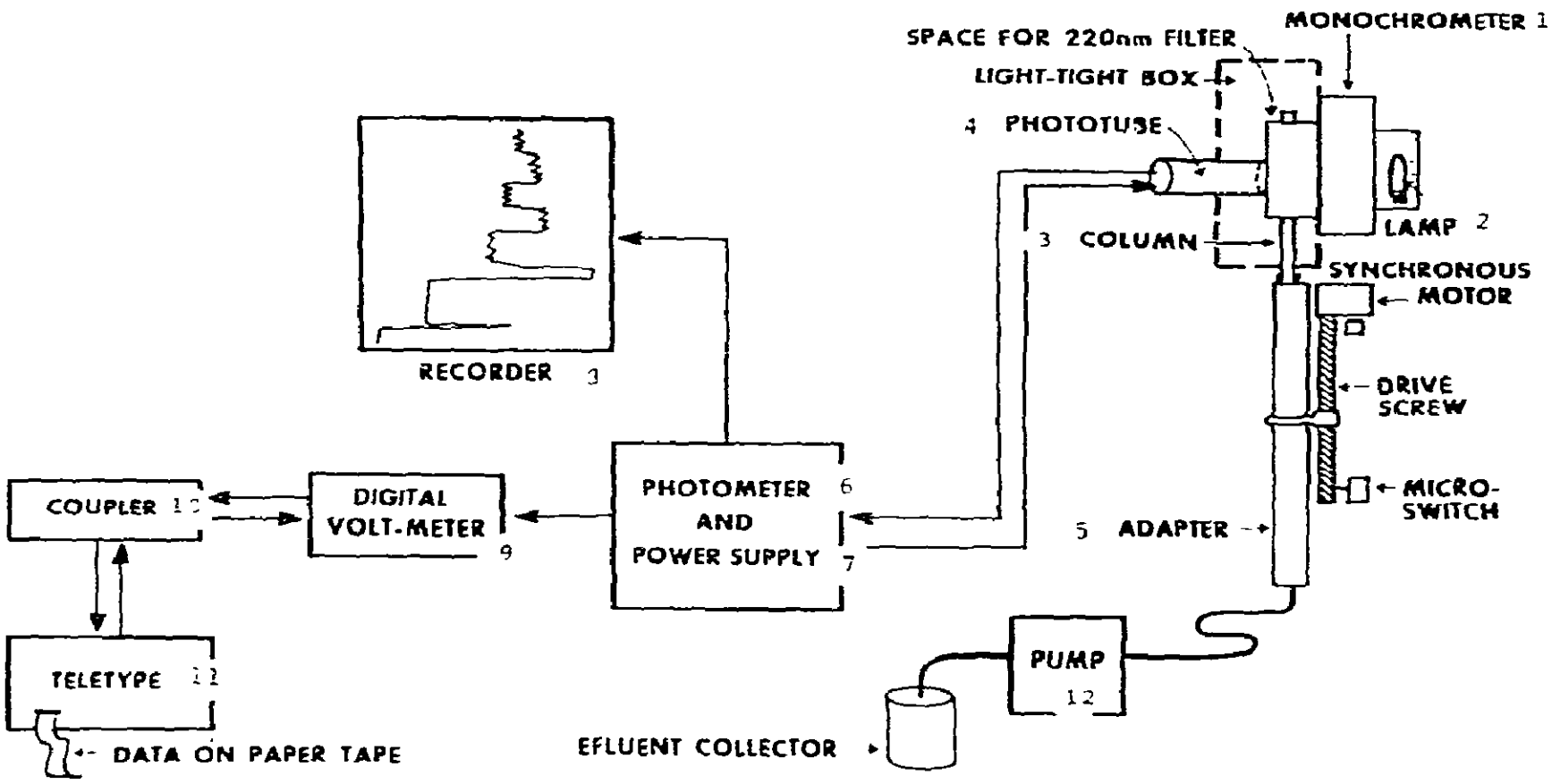
MONOCHROMETER 1
SPACE FOR 220nm FILTER
LIGHT-TIGHT BOX
4 PHOTOTUBE
LAMP 2
3 COLUMN
SYNCHRONOUS MOTOR
DRIVE SCREW
MICRO-SWITCH
5 ADAPTER
RECORDER 3
PHOTOMETER AND POWER SUPPLY 6 7
DIGITAL VOLT-METER 9
COUPLER 10
TELETYPE 11
DATA ON PAPER TAPE
PUMP 12
EFLUENT COLLECTOR

(a)

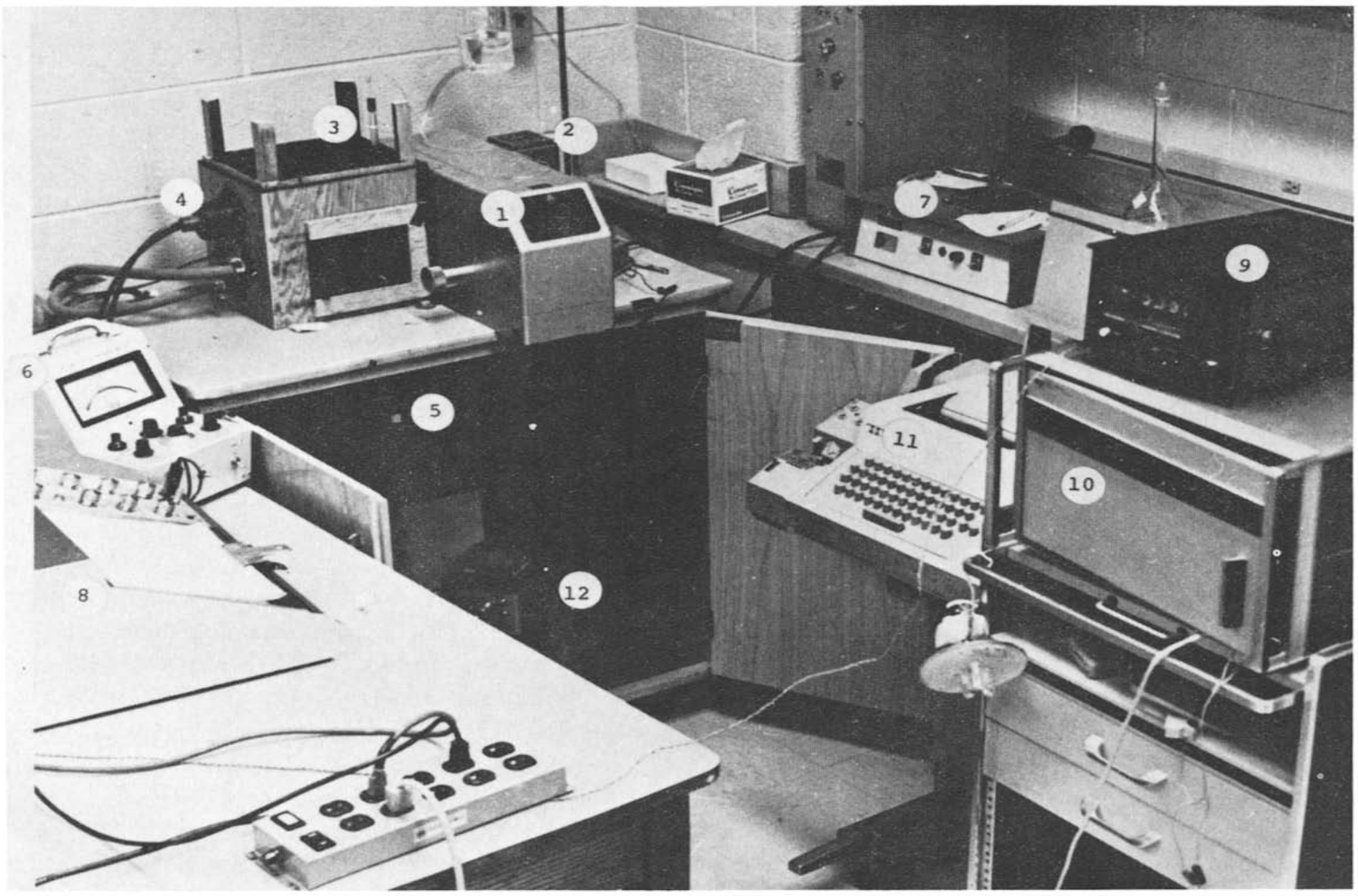
1
2
3
4
5
6
7
8
9
10
11
12

(b)

partition cross sections. Use of these transport parameters in providing inferences regarding molecular properties are well-established [5] and will not be discussed here. In an accompanying paper we describe the application of these methods to active enzyme transport. Detailed analyses of solute profile shapes for self-associating solutes will be described in a later paper.

The technique of scanning gel chromatography is particularly well-suited for studies of protein solutes at low concentration, since the measurements can readily be made at 220 nm, where the extinction coefficients are very high (e.g., by a factor of approximately ten compared with values at 280 nm for many proteins) [13].

## 2. Experimental

### 2.1. Materials

All gel chromatography experiments were performed on Sephadex G-200 obtained from Pharmacia. Marker proteins were purchased commercially. Glycylglycine and the holoenzyme of rabbit muscle glyceraldehyde-3-phosphate dehydrogenase were obtained from Sigma. Sperm whale myoglobin was from Mann. The void volume marker blue dextran was obtained from Pharmacia. Tobacco mosaic virus was a gift of Dr. Robert Scheele, (Department of Biology, University of Connecticut). Hemoglobin was prepared from freshly drawn blood by the method of Williams and Tsay [14].

### 2.2. Instrumentation

The scanning chromatograph used in these studies has previously been described [1]. It was equipped with a digital data acquisition system and an LKB Varioperpex pump which maintained a constant flow rate of approximately 3.0 ml per hour. The arrangement of the scanning equipment and the data acquisition tion system is shown in fig. 1.

### 2.3. Photometric performance

The necessity of determining solute absorbances with precision at 220 nm above a high baseline (due to light scattering by the gel) places very severe demands upon the photometric accuracy of the scanning chromatograph. In order to minimize stray light from remote wavelengths, an interference filter with a maximum transmittance at 220 nm was mounted just in front of the photomultiplier. Beer's law tests at 220 nm then showed strictly linear behavior to within measureable limits up to an optical density of 2.3. Minor corrections could accurately be applied up to absorbances of 3.2. Photometric precision was generally better than ±0.001 absorbance units at an optical density of 1.5.

### 2.4. Columns

The quartz column (17 cm ×0.945 cm) was packed under gravity with Sephadex G-200, previously swollen in 0.1 M potassium phosphate buffer, pH 7.6 Glass wool served as the base on which the gel bed was packed A porous polyethylene disc was used to stabilize the top of the column.

### 2.5. Single solute profile determinations

Experiments of the large zone type [5] were carried out with monodisperse solutes according to the follow ing procedures. The gel column was equlibrated with 0.25 M potassium phosphate buffer, pH 7.6, with $10^{-4}$M EDTA and repeatedly scanned until a reproducible baseline was obtained. The criterion for the reproducibility of all saturation scans was established to be that the mean difference in absorbance at each point in the column between two consecutive scans not exceed 0.0015. In practice the mean of differences between any two scans used seldom exceeded 0.0010 absorbance units. Three scans which met such criteria were averaged to yield a reference baseline or saturation scan.

Protein solutions were made to approximately 0.1 mg/ml in 0.25 M phosphate buffer and filtered twice through No. 2 filter paper. The inside of the column above the disc was rinsed several times with the protein solution before the column was actually filled and column loading begun. At the instant the column saturation was started a timer was started to

Fig. 1. Scanning gel chromatograph used in determining solute profiles. (a) Schematic diagram, (b) photograph. Numbers correspond to components shown in scheme (a).

record the initial time ($t_0$) and to follow the time course of the saturation.

The column was repeatedly scanned to observe the development of the leading boundaries of the saturation species. As each scan was initiated, the time since $t_0$ was noted. The absorbance at each point in the column was monitored visually using a Sargent SRL recorder which yielded a tracing of each scan. The actual transmittance data were punched on paper tape for subsequent numerical analysis.

When the absorbance at all points in the gel reached a maximum, the column was scanned several times to obtain a reproducible protein saturation profile. The region of the column above the disc was then rinsed with filtered phosphate buffer and re-equilibration of the column with buffer was begun. Repeated scans were made to observe the trailing boundary as the sample moved out of the column.

Finally, after all sample had been eluted, a post-experiment phosphate buffer baseline was obtained. In most cases, this post baseline was used in conjunction with the saturated protein scan to determine the species partition cross-section.

### 2.6. Associating solute profile determinations

Experiments with carboxyhemoglobin were carried out using procedures similar to those described above for the noninteracting solute profile determinations. These experiments were done with a series of samples covering a range of hemoglobin concentration between 2 μg/ml and 400 μg/ml. At the highest concentration (above 90 μg/ml) scans were performed at 240 nm. All other measurements were made at 220 nm.

## 3. Analysis of solute profiles

### 3.1. Data processing

Transmittance data recorded on punched paper tapes were read into a Hewlett-Packard 2114A digital computer equipped with high speed photoreader and punch. Using an interactive program it was possible to determine the reproducibility of buffer and reagent baseline scans, as well as saturated protein scans, to average reproducible scans, and to produce reference baseline and protein scans in terms of absorbances; to punch tapes of the partition cross section ($\xi$) at every point in the gel bed; to determine the partition coefficient ($\sigma$) for partially included species; to print out baseline-subtracted records of the absorbance at every point in the column for each scan; and to calculate the average baseline drift over regions of the column into which the profile has not progressed.

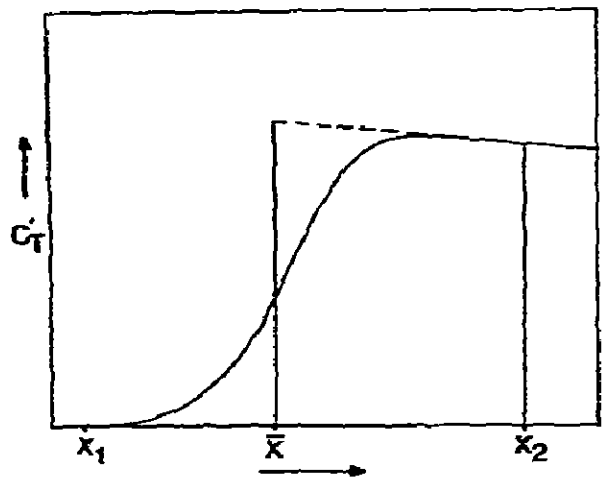


Fig. 2. Diagram of trailing boundary in large zone experiment. $X_1$ and $X_2$ are arbitrary reference positions within the buffer baseline and solute plateau, respectively. $\bar{X}$ is the centroid calculated according to eq. (4a).

### 3.2. Calculation of centroids

The essential information to be obtained from each profile is the centroid $\bar{X}$. The rate of movement of the centroids is related to the partition cross section, $\xi$, by the fundamental relationship:

$$d\bar{X}/dt = F/\xi A, \tag{1}$$

where $F$ is the volume flow rate and $A$ is the column's cross-sectional area. The partition cross section represents the fraction of $A$ which is accessible to solute. This quantity $\xi$ is dependent on position $X$ within the gel bed. A typical boundary profile for the trailing boundary in a large zone experiment is diagramed in fig. 2 where $X_1$, $X_2$ represent arbitrary points of the baseline and in the plateau, respectively. The slanted "plateau" represents the variation of $\xi$ with position. The total mass $Q$ of solute contained between $X_1$ and $X_2$ is represented by the integral of the solute concentration $C'$ (i.e., mass per unit volume of column bed) over the differential volume elements $A\,dx$:

$$Q = \int_{X_1}^{X_2} C' A \, dX. \tag{2}$$

The centroid position ($\bar{X}$) is defined so that the total amount of solute at the plateau concentration $C_0$ between $X_2$ and $\bar{X}$ would equal $Q$. $Q$ therefore is the product of the initial loading concentration of solute $C_0$ and the volume of gel available to the solute between $\bar{X}$ and $X_2$:

$$Q = C_0 \int_{\bar{X}}^{X_2} \xi(X)\, A\, dX. \tag{3}$$

Both $C_0$ and the partition cross section $\xi$ are obtained from the averaged buffer baselines and averaged protein saturation scans for the single solute species [1]. When the column is completely saturated with solution containing the solute of interest, the measured absorbance $A_b$ at any point within the gel bed (i.e., after baseline subtraction) is related to the concentration $C'$ (i.e., *within the column*) by the Beer's Law relationship: $A_b = \epsilon C' l$ where $\epsilon$ and $l$ are the extinction coefficient and pathlength respectively. Similarly, for the solution above the gel bed $A_a = \epsilon C_0 l$. The ratio $A_b/A_a$ equals the partition cross section $\xi(1)$.

The centroid $\bar{X}$ is calculated for each trailing profile by determining (by numerical integration) values of the integrals in the following relationship:

$$\int_{\bar{X}}^{X_2} \xi(x)\, dX = (1/C_0) \int_{X_1}^{X_2} C'\, dX. \tag{4a}$$

For a leading boundary similar considerations apply and the formula corresponding to (4a) is:

$$\int_{X_1}^{\bar{X}} \xi\, dX = (1/C_0) \int_{X_1}^{X_2} C'\, dX. \tag{4b}$$

Centroids calculated from a series of scans taken at various times for a moving boundary can be used to calculate apparent rates of motion and partition cross sections according to eq. (1). However more accurate values are obtained by first making the following correction.

### 3.3. Time frame profile correction

Profiles determined by direct scanning of gel columns are dynamic profiles. The absorbance at each point in the gel is determined at a different time from every other point and the profiles continue to develop even as they are scanned. The net result is that the centroid determined for any given profile relates to no fixed time frame. However, if the profile distortion arising from finite rate of scanning is small, a good approximate correction can be made to the profile's shape and position within the column using the following procedure:

Since the rate of scanning and the rate of motion of the profile, as defined by the rate of motion of the centroid, are known, the position within the column of each point on the profile may be corrected to a fixed time (for example the time at which the scan was begun) by the equation:

$$X' = XS(1 - V_c/R), \tag{5}$$

where the corrected distance coordinate $X'$ is related to the initially determined value $X$, the distance $S$ per data point (0.458 mm in the present case), the scan rate $R$ (0.832 mm/s) and the rate of motion $V_c$ of the centroid (mm/s). An initial value of $V_c$ is determined from the rate of motion of centroids determined by eq. (4a,b) for the experimentally measured series of scans. The correction is then applied to each point within the profile.

This correction procedure does not change the data point number of the profile centroid, but does alter the value assigned to its distance within the column, as well as the time required to reach that position. Consequently, a new rate of motion $V_c$ is determined, and a further correction of centroid position made. A program was written to make these corrections on the solute profiles successively until no further change occurred in the rate of motion of the centroid. The resulting boundary profile then approximates that of an instantaneous scan taken at $t_0$.

## 4. Results

### 4.1. Noninteracting solutes

Boundary profile determinations were made for the experiments with glycylglycine, sperm whale myoglobin, rabbit muscle glyceraldehyde-3-phosphate dehydrogenase and tobacco mosaic virus. Plots of baseline-subtracted (but uncorrected) scans of leading and trailing boundaries are shown in fig. 3. It can be seen that the boundaries are well-defined with little scatter in the

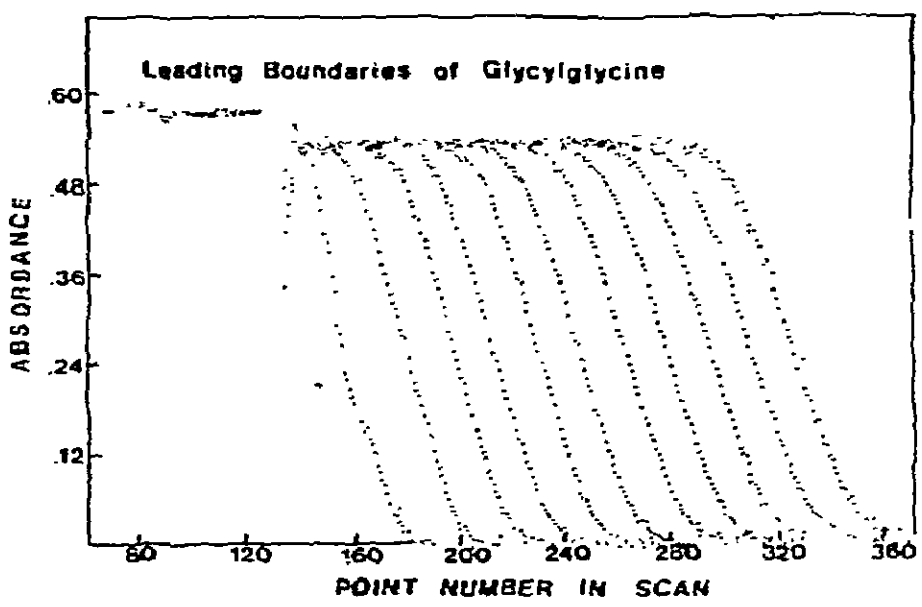


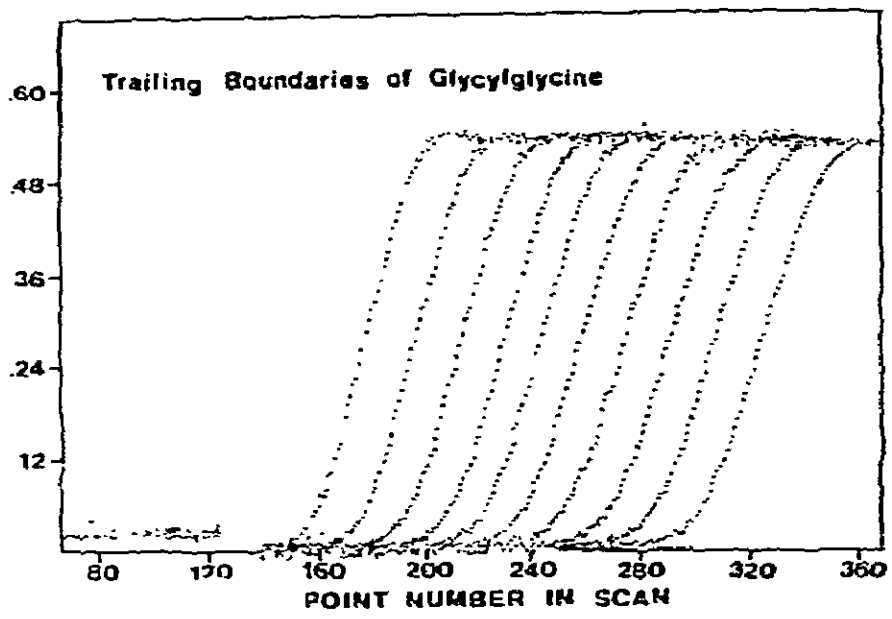


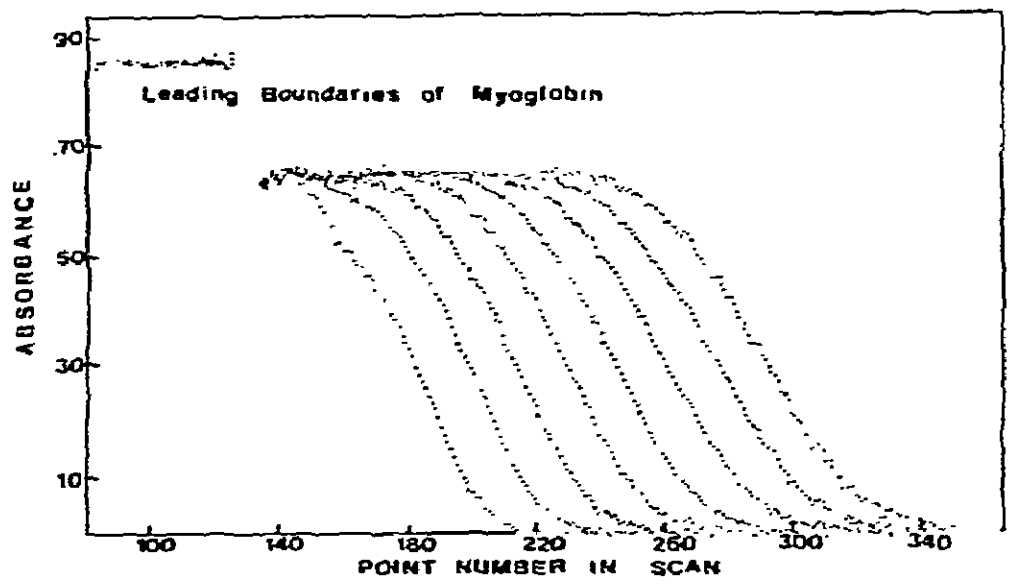


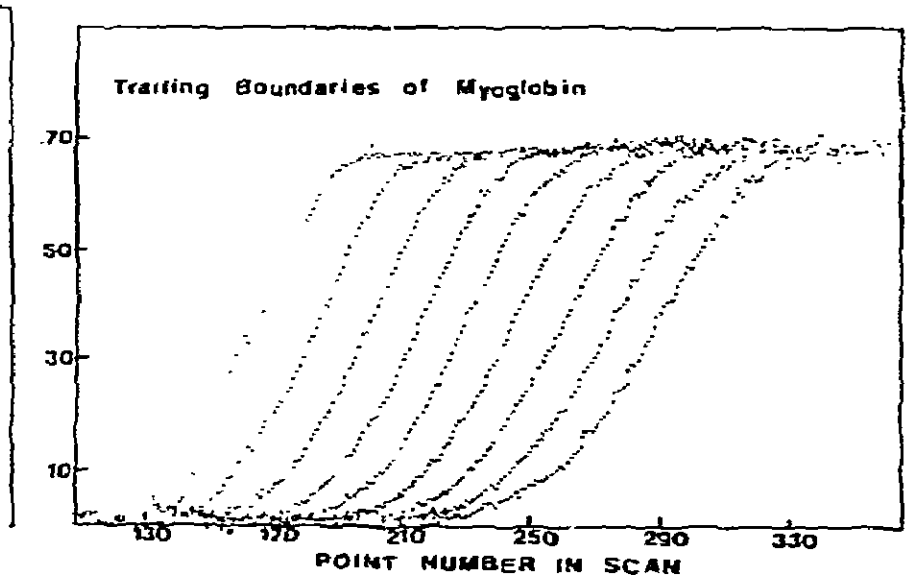


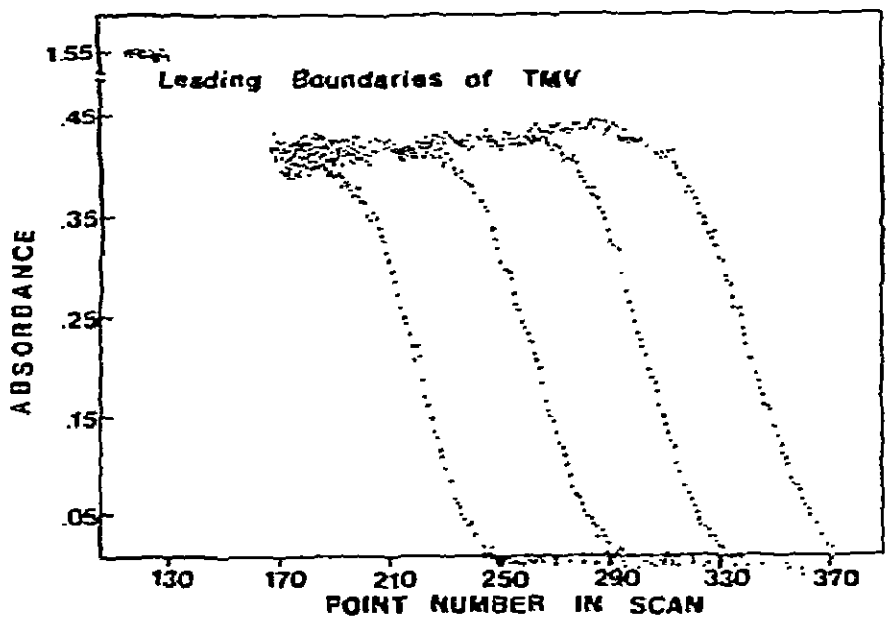


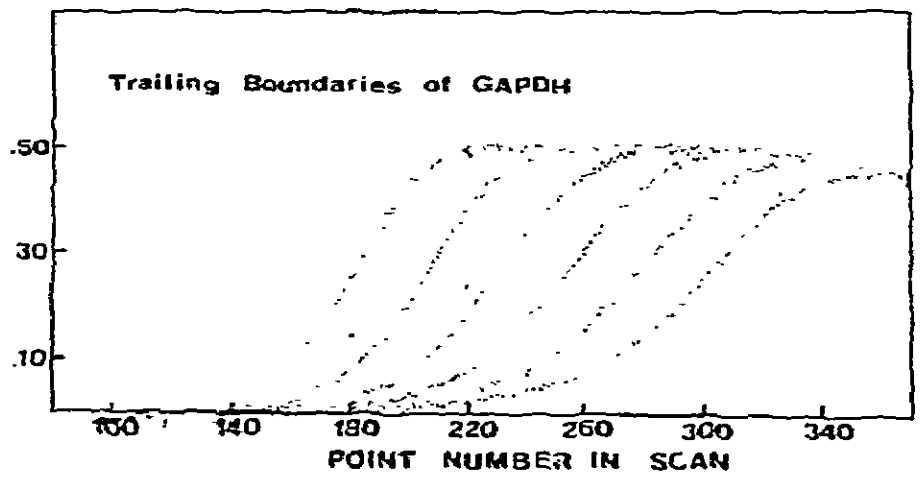


Fig. 3. Baseline-subtracted scans of noninteracting solutes on a Sephadex G-200 column. For leading boundaries the envelope of points at the upper left denotes the protein solution absorbance above the column bed. The distance between each point number corresponds to 0.458 millimeters. The optical scanning window is 1 mm in height. Scans were made at 220 nm, and are not corrected to constant time frame.

Table 1
Correction of centroid position to the time frame $t_0$

| Centroid position $\bar{X}$ (mm) | $t_0$ (s) | Corrected centroid $\bar{X}'$ (mm) | Rate of centroid motion (mm/s) |
|---|---|---|---|
| Glycyl–glycine – Leading boundaries | | | |
| 20.52 | 1653 | 20.21 | 0.0122 |
| 28.82 | 2319 | 28.39 | 0.0124 |
| 35.42 | 2839 | 34.90 | 0.0123 |
| 43.16 | 3470 | 42.53 | 0.0121 |
| 50.07 | 4012 | 49.32 | 0.0125 |
| 58.16 | 4664 | 57.30 | 0.0122 |
| 65.28 | 5216 | 64.29 | 0.0126 |
| 72.84 | 5830 | 71.77 | 0.0122 |
| 79.84 | 6404 | 78.69 | 0.0120 |
| 87.06 | 6987 | 85.78 | 0.0122 |
| Glycyl–glycine – Trailing boundaries | | | |
| 3.80 | 318 | 3.75 | 0.0118 |
| 11.23 | 920 | 11.07 | 0.0121 |
| 19.98 | 1596 | 19.67 | 0.0127 |
| 28.32 | 2264 | 27.90 | 0.0123 |
| 35.75 | 2871 | 35.23 | 0.0121 |
| 43.06 | 3464 | 42.44 | 0.0121 |
| 49.29 | 3971 | 48.57 | 0.0121 |
| 56.09 | 4511 | 55.26 | 0.0124 |
| 63.25 | 5093 | 62.33 | 0.0121 |
| 71.26 | 5705 | 70.16 | 0.0128 |
| 78.73 | 6295 | 77.55 | 0.0125 |
| 86.94 | 6926 | 85.60 | 0.0128 |
| Myoglobin – Leading boundaries | | | |
| 20.34 | 1222 | 19.95 | 0.0163 |
| 27.78 | 1671 | 27.24 | 0.0162 |
| 34.61 | 2116 | 33.98 | 0.0151 |
| 42.04 | 5282 | 41.25 | 0.0156 |
| 48.97 | 3032 | 48.07 | 0.0152 |
| 55.79 | 3494 | 54.81 | 0.0146 |
| 63.22 | 3946 | 62.01 | 0.0159 |
| 69.96 | 4393 | 68.70 | 0.0150 |
| 76.98 | 4840 | 75.56 | 0.0154 |
| Myoglobin – Trailing boundaries | | | |
| 14.08 | 790 | 13.78 | 0.0174 |
| 21.36 | 1239 | 20.95 | 0.0160 |
| 27.58 | 1692 | 27.12 | 0.0136 |
| 34.51 | 2139 | 33.88 | 0.0151 |
| 41.29 | 2580 | 40.54 | 0.0151 |
| 48.13 | 3029 | 47.26 | 0.0150 |
| 55.16 | 3483 | 54.15 | 0.0152 |
| 62.07 | 3928 | 60.93 | 0.0152 |
| 68.75 | 4366 | 67.51 | 0.0150 |
| Glyceraldehyde-$PO_4$ dehydrogenase – Leading boundaries | | | |
| 21.40 | 778 | 20.71 | 0.0266 |
| 32.71 | 1218 | 31.73 | 0.0250 |
| 44.04 | 1665 | 42.74 | 0.0246 |
| 55.17 | 2111 | 53.56 | 0.0242 |
| 66.28 | 2561 | 64.37 | 0.0240 |
| 77.70 | 3010 | 75.40 | 0.0246 |
| Glyceraldehyde-$PO_4$ dehydrogenase – Trailing boundaries | | | |
| 9.26 | 325 | 8.96 | 0.0276 |
| 21.24 | 773 | 20.58 | 0.0259 |
| 32.05 | 1217 | 31.14 | 0.0237 |
| 42.74 | 1662 | 41.53 | 0.0234 |
| 53.12 | 2109 | 51.68 | 0.0227 |
| 63.54 | 2554 | 61.81 | 0.0227 |
| 73.96 | 3001 | 71.94 | 0.0227 |
| Tobacco mosaic virus – Trailing boundaries | | | |
| 34.95 | 673 | 32.89 | 0.0489 |
| 53.90 | 1112 | 51.20 | 0.0418 |
| 73.10 | 1558 | 69.47 | 0.0413 |
| 92.08 | 1999 | 87.55 | 0.0409 |

points to obscure their shape. In general, both leading and trailing boundaries appear symmetrical. Increased boundary spreading (axial dispersion) as the sample moves down the column is evident, as is the pronounced effect of molecular size on boundary spreading. As expected [15] the larger non-excluded solutes exhibit greater rates of axial dispersion. It should be noted also that the plateau values are very smooth with very small slopes, indicating nearly uniform column packing.

Table 1 is a compilation of corrected centroids and their rates of motion. The corrected centroids are listed in terms of the number of millimeters they have moved into the gel bed. As one would have expected, the time-corrected centroid position corresponds to a shorter distance within the gel bed and the magnitude of the correction is greater for the more rapidly moving solutes

In order to illustrate how this correction alters the shape of an entire profile, the seventh scan of the leading boundary of myoglobin has been adjusted at every point to the time the scan was initiated and is shown in fig. 4 along with the uncorrected scan. The rate of

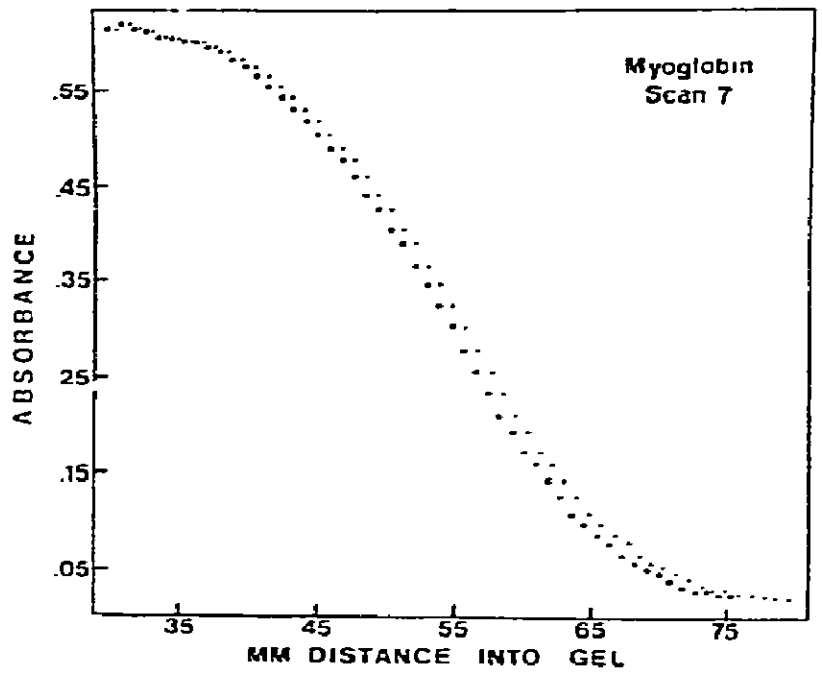


Fig. 4. Correction of boundary profile to constant time frame, eliminating the effect of finite column scanning rate. (o) Experimentally determined profile, (X) corrected profile.

motion of the corrected centroid of that scan was used in computing the new position of each point. The profile's shape for myoglobin (molecular radius 18.8 Å) is seen to be small. Indeed, the correction is not major for a species like TMV, which is totally excluded from the gel. Validity of the correction procedure depends upon there being only a small distortion in the measured profile shape.

The ultimate value of being able to determine accurately the centroid positions and rates of motion of dynamic profiles is in relating these motions to molecular size, i.e., through the molecular size-dependent partition cross section $\xi$. The additional data necessary for this calculation are the cross-sectional area of the column and the solvent flow rate. For these single solute experiments, a single column was used throughout and the area was 0.715 $cm^2$. The flow rate was determined independently for each species, often independently for both leading and trailing boundaries. The partition cross section calculated in this way for the centroid position of each scan is compared with the partition cross section determined by protein saturation data in Table 2 for myoglobin.

It can be seen that the deviation of $\xi$'s determined from centroid movement relative to "true" saturation $\xi$'s was small (less than 4% at all points considered). These and similar results serve to establish that the rates of centroid motion for profiles observed by the direct optical scanning technique can be used to obtain valid determinations of fundamental molecular size-dependent transport parameters.

Table 2
Determination of partition cross sections by two methods with myoglobin on a Sephadex G-200 column

| Distance from top of gel bed $\bar{X}$ (mm) | Rate of centroid motion (mm/s) | Partition cross section $\xi$ | |
|---|---|---|---|
| | | A. From centroid rate[a] | B. From saturation |
| 19.95 | 0.0163 | 0.735 | 0.787 |
| 27.24 | 0.0162 | 0.739 | 0.790 |
| 33.98 | 0.0151 | 0.792 | 0.792 |
| 41.25 | 0.0156 | 0.770 | 0.791 |
| 48.07 | 0.0152 | 0.789 | 0.804 |
| 54.81 | 0.0146 | 0.823 | 0.799 |
| 62.01 | 0.0159 | 0.753 | 0.805 |
| 68.70 | 0.0150 | 0.801 | 0.804 |
| 75.56 | 0.0154 | 0.780 | 0.805 |

[a] Calculated from leading boundary data.

### 4.2. Estimation of axial dispersion coefficients

In addition to the partition cross section which determines the average rate of translational motion of a solute within the column, it is of interest to calculate the axial dispersion coefficient $L$. This parameter also depends upon molecular size and determines the rate of spreading of the solute boundary [15]. Since the scans exhibited nearly flat plateaus, approximate values of $L$ could be calculated from the profiles according to the formula [15]:

$$L = \frac{1}{4\xi^2 A^2 t}\left\{\frac{\xi AX - Ft}{\operatorname{erfc}^{-1}(2C'/C_0')}\right\}^2. \qquad (6)$$

Typical results for this type of calculation are those of myoglobin which yielded a value of $(2.35 \pm 0.7) \times 10^{-4}$ $cm^2/s$ for $L$.

### 4.3. Carboxyhemoglobin

Trailing boundaries of human carboxyhemoglobin solutions are shown in fig. 5 as a function of plateau concentration. The objective of these studies was twofold; (1) to explore the lowest concentration limits of the technique and (2) to illustrate the characteristic

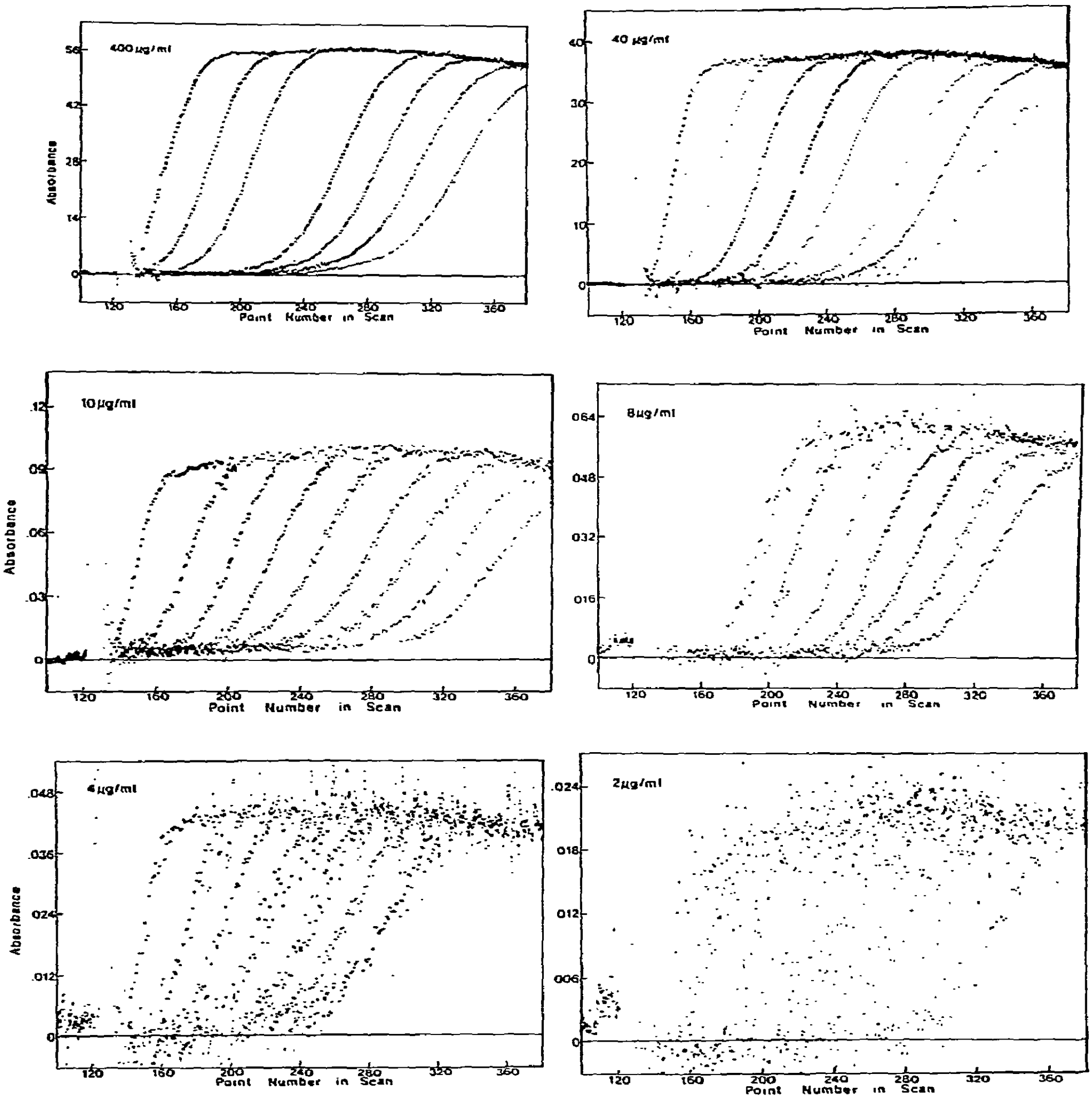


Fig. 5. Trailing boundaries of human carboxyhemoglobin on Sephadex G-200 column. Boundaries were scanned at 220 nm except for the highest concentration where $\lambda = 240$ nm.

boundary shapes and concentration-dependent centroid rates for a self-associating solute.

The effect of protein concentration on resolution of boundaries from scans taken at 220 nm is vividly illustrated by the results shown in fig. 5. In the lowest concentration ranges the r.m.s. noise is approximately constant at ±0.001 absorbance units. This imposes a severe limitation on resolution of boundary shapes at concentrations below about 5 μg/ml, although approximate boundary positions (centroids) are still obtainable from the data at 2 μg/ml. It should be noted that these protein absorbances are measured above a baseline optical density (due to light scattering by the gel) of about 1.5. Results of the quality presented here can only be achieved with an instrument of exceptionally high photometric accuracy in the low wavelength ranges.

The hemoglobin trailing boundary profiles are asymmetric, as expected for a self-associating solute (cf. ref. [5]) and also exhibit concentration dependent rates of centroid motion. The boundaries, although skewed, are unimodel, as expected for a dimer–tetramer association stoichiometry. The partition cross-section for a self-associating solute is a weight average of the species ξ's [5] and its variation with total protein concentration generates a dissociation curve shown in fig. 6. These weight average ξ's were calculated according to eq. (1). The solid curve (fig. 6) is a fitted dissociation curve corresponding to an equilibrium constant of 160.5 $d\ell/g$, end-points of 0.542 (tetramer) and 0.724 (dimer), and a nonideality term ($g = -0.15$). The data are insufficient to define the above four parameters simultaneously with precision and are presented here only to illustrate the types of variation observed. A subsequent paper will include more extensive data of this type and will deal with the problem of detailed analyses for stoichiometry and equilibrium constants.

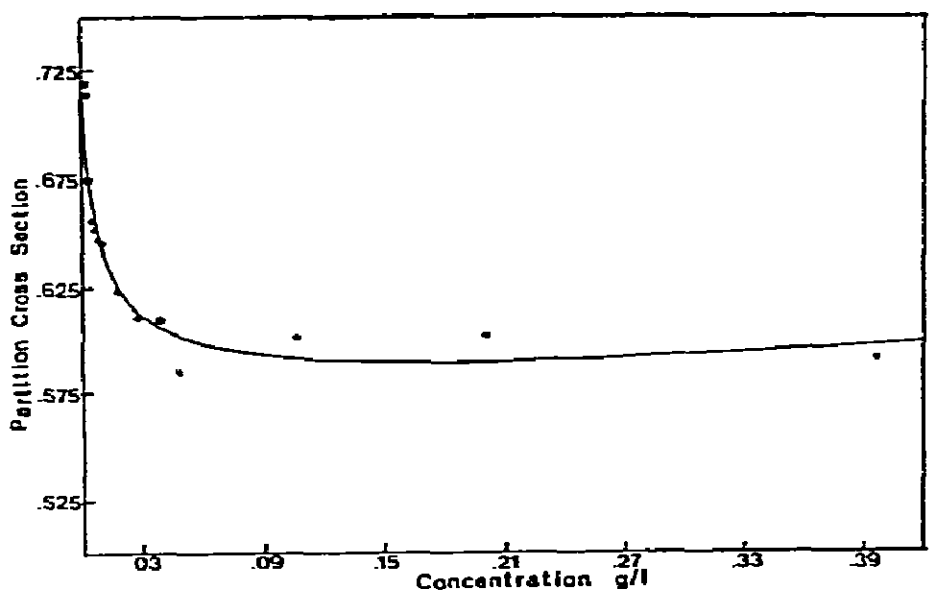


Fig. 6. Concentration dependence of partition cross sections for carboxyhemoglobin calculated from rates of centroid motion.

## 5. Discussion

This study has been aimed primarily at exploring the feasibility and limits of accuracy whereby boundary profiles may be determined using the technique of scanning gel chromatography. We have placed primary emphasis upon the goal of determining reliable partition cross sections from rates of centroid motion within the column. Although this basic phenomenological parameter can be determined most accurately from equilibrium saturation experiments, its determination from dynamic considerations is of great interest for applications to the technique of active enzyme gel chromatography, described in accompanying papers [11,12].

The results of experiments presented here establish that good agreement exists between partition cross sections determined by dynamic and equilibrium approaches. Rate of motion studies with molecular species of widely differing molecular weight, e.g., glycylglycine (132) and glyceraldehyde-3-phosphate dehydrogenase (156 000) yielded partition cross sections which were found to agree closely with corresponding cross sections obtained by the equilibrium saturation method. The agreement was always within 4%. Since the calculation of centroid positions and partition cross sections from their rate of motion is based exclusively on conservation of mass considerations, there is no reason in principle to expect anything less than complete agreement between these ξ's and those calculated from the equilibrium saturation method. We have observed that minor manipulations of the reference baseline, i.e., on the order of 0.001 absorbance units (the scan reproducibility limits) can cause substantial changes in the saturation ξ, while barely altering the ξ from the centroid rate of motion. In the results presented here such manipulations have been avoided. Nor was any smoothing of the data carried out.

It should be noted that obtaining an accurate value for the absorbance of the solution above the disc is also crucial to the accurate determination of centroids. In most instances this solution absorbance was found to differ slightly when new protein solution was added to the column during the experiment. Although this source of error may be minimized, it is difficult to eliminate entirely.

It is interesting that in the present studies the columns produced remarkably constant partition cross sections throughout their entire length. In many cases, the beads of gel pack more closely at the bottom, reducing the void volume fraction by several percent [1] and changing the transport behavior as protein moves down the column. This effect is very minor in the present study, making eq. (6) a good approximation for calculation of axial dispersion coefficients. In other cases no such simple formula can be applied.

The carboxyhemoglobin results illustrate the applicability of the technique to self-associating solutes and also serve to define the lower limits of protein concentration to which the methods can be applied. This limit appears to be approximately 2 $\mu$g/ml (0.12 micromolar in heme). In a subsequent paper we will describe studies of detailed boundary shapes for such a self-associating solute system. The application of results obtained here to the study of active enzyme transport is described in the accompanying paper [11].

## Acknowledgement

We are grateful to Dr. David J. Cox for highly beneficial modifications to the scanning gel chromatograph carried out during a sabbatical visit in our laboratory and to Dr. Michael L. Johnson for valuable help in the development of computer programs for analyses described in this paper.

## References

[1] E.E. Brumbaugh and G.K. Ackers, J. Biol. Chem. 244 (1968) 6315.
[2] E.E. Brumbaugh and G.K. Ackers, Anal. Biochem. 41 (1971) 543.
[3] H.W. Warshaw and G.K. Ackers, Anal. Biochem. 42 (1971) 405.
[4] G.K. Ackers, E.E. Brumbaugh, S.H.C. Ip and H.R. Halvorson, Biophys. Chem. 4 (1976) 171.
[5] G.K. Ackers, in: The Proteins, Third Ed., Vol. 1, eds. H. Neurath and R.L.Hill (Academic Press, New York, 1975) p. 1.
[6] L.M. Gilbert and G.A. Gilbert, in: Methods of Enzymology, Vol. XXVII, Part D, eds. C.W.H. Hirs and S.N. Timasheff (Academic Press, New York, 1973).
[7] J.K. Zimmerman and G.K. Ackers, J. Biol. Chem. 246 (1971) 1078.
[8] J.K. Zimmerman, D.J. Cox and G.K. Ackers, J. Biol. Chem. 246 (1971) 4242.
[9] J.K. Zimmerman and G.K. Ackers, J. Biol. Chem. 246 (1971) 7289.
[10] H.R. Halvorson and G.K. Ackers, J. Biol. Chem. 249 (1974) 967.
[11] M.M. Jones, J.W. Ogilvie and G.K. Ackers, Biophys. Chem. 5 (1976) 339.
[12] B.B. Brown and J.K. Zimmerman, Biophys. Chem. 5 (1976) 351.
[13] G.C. Webster, Biochem. Biophys. Acta 207 (1970) 371.
[14] R.C. Williams, Jr. and K. Tsay, Anal. Biochem. 54 (1973) 137.
[15] H.R. Halvorson and G.K. Ackers, J. Polymer Sci. A-2 9 (1971) 245.